Available online at www.sciencedirect.com
ScienceDirect
Image and Vision Computing 26 (2008) 971–979
www.elsevier.com/locate/imavis

Multifocus image fusion using region segmentation and spatial frequency

Shutao Li *, Bin Yang

College of Electrical and Information Engineering, Hunan University, Changsha 410082, China

Received 20 September 2006; received in revised form 20 June 2007; accepted 31 October 2007

Abstract

Image fusion is a process of combining complementary information from multiple images of the same scene into an image, so that the resultant image contains a more accurate description of the scene than any of the individual source images. In this paper, a new region-based multifocus image fusion method is proposed. The motivation of our proposed method lies in the fact that region-based image fusion methods could be more meaningful than pixel-based fusion methods which just consider individual pixels or associated local neighborhoods of pixels in the fusion process. The fusion process contains the following steps: firstly, multifocus images are fused using the simple average method. Then the intermediate fused image is segmented using the normalized cut method. Then the two source images are segmented according to the segmenting result of the intermediate fused image. Finally, the corresponding segmented regions of the source images are fused according to their spatial frequencies. Experimental results on several pairs of multi-focus image show that the proposed method can give good results. The proposed method is more robust to misregistration or slight motion of the object than the pixel-based method.

Keywords: Image fusion; Image segmentation; Normalized cuts; Multi-focus; Digital cameras

1. Introduction

In applications of digital cameras, when a lens focuses on a subject at a certain distance, all subjects at that distance are sharply focused. Subjects not at the same distance are out of focus and theoretically are not sharp. Fig. 1 shows a geometric optical model of image formation. Suppose that the lens focuses on the dot 'A', a dot 'a' will be generated on the image plane. Once focused, all subjects that have the same subject-lens distance as that of the 'A' dot will appear sharp. Now, consider a dot 'B' that is behind the dot 'A' (i.e., with larger subject-lens distance). Since it is out of focus, it will not produce a sharp dot 'b'. Instead, its image is formed somewhere in front of the image plane. On the image plane, the image of this dot 'B' is a circle as shown in Fig. 1. This circle is usually referred to as the circle of confusion. As the subject-lens distance increases, the size of this circle increases. The same holds true for a subject in front of the dot 'A' (e.g., the dot 'C' in Fig. 1). The zone of acceptable sharpness is referred to as the depth of field. One would like to acquire images that have large depth of field, i.e., the images are in focus everywhere. A possible way to solve this problem is by image fusion, in which one can acquire a series of pictures with different focus settings and fuse them to produce an image with extended depth of field [2–4]. This fused image will then hopefully contain all the relevant objects in focus.

The simplest image fusion method just takes the pixel-by-pixel gray level average of the source images. This, however, often leads to undesirable side effects such as reduced contrast [1,2]. Multiscale transforms are very useful for analyzing the information content of images for fusion purposes. Various methods based on the multiscale transforms have been proposed, such as Laplacian pyramid-based,

* Corresponding author. Tel.: +86 731 8672916; fax: +86 731 8822224.
E-mail addresses: shutao_li@yahoo.com.cn (S. Li), yangbin01420@163.com (B. Yang).

0262-8856/$ - see front matter © 2007 Elsevier B.V. All rights reserved.
doi:10.1016/j.imavis.2007.10.012

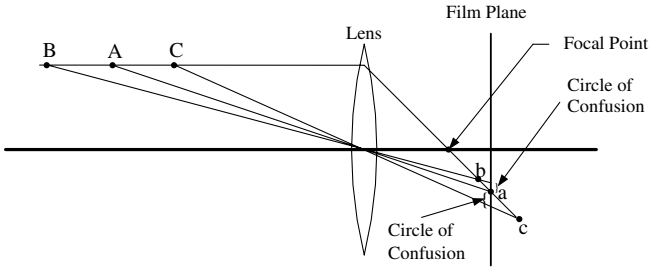

Fig. 1. Geometric optics model.

gradient pyramid-based, ratio-of-low-pass pyramid-based, discrete wavelet-based (DWT) [3–14]. The basic idea is to perform a multiresolution decomposition on each source image, then integrate all these decompositions to form a composite representation, and finally reconstruct the fused image by performing an inverse multiresolution transform. In recent years, some extensions to the classical wavelet transform have been used for image fusion. The discrete multiwavelet transform based image fusion methods are proposed in reference [15,16]. The multiwavelet offers the advantages of combining symmetry, orthogonally, and variable support, which cannot be achieved by scalar two-channel wavelet systems at the same time. Ishita De proposed a decomposition scheme which is based on a nonlinear wavelet constructed with morphological operations and presented a multifocus image fusion algorithm using this decomposition scheme [17]. This method is suitable for hardware implementation because of its simple arithmetic operations, however, artifacts may be formed in the fused image.

One limitation of pixel or decomposition coefficients based methods is that they are sensitive to noise or misregistration. Therefore, some researchers proposed to fuse images using region-based methods [18–20], in a wavelet decomposition framework. First, pre-registered images are transformed using a multiresolution analysis method. Regions representing image features are then extracted from the transform coefficients by an image segmentation method. The regions are then fused based on region characteristics. Experimental results of these methods are encouraging. However, image fused in this way may still lose some information of the source images because of the implementation of the inverse multiresolution transform.

In this paper, we propose an effective algorithm which is implemented in the spatial domain and is suitable for combining multi-focus images of a scene. The intuitive idea is that images are perceived by humans in the region or object level instead of pixel level. It contains three steps: image segmentation, region clarity calculation and fused image construction. The first step of the proposed method is to fuse the two source images by simple averaging. Then the fused image is segmented by normalized cuts. Using this result, the two source images are partitioned. Finally, the corresponding regions of the two source images are fused using the spatial frequency measure.

The segmentation results are vital to the final fusion result as the whole implementation is based on the segmented region. Shi et al. proposed a novel approach for solving the perceptual grouping problem in vision [21]. Rather than focusing on local features, the approach aims at extracting the global information of an image. The image segmentation process was treated as a graph partitioning problem and a novel global criterion, normalized cut, was proposed for segmenting the graph. The normalized cut criterion can measure both the total dissimilarity and the total similarity within different groups. The normalized cut based image segmentation method was adopted in our proposed image fusion algorithm.

In practice, the images are usually captured by a handheld or mobile camera, and fusion of the images requires registration of the images prior to fusion [22]. Registration is a fundamental task in image processing. It is the process of spatially aligning two or more images of a scene. The processing brings into correspondence individual pixels in the images. Therefore, given a point in one image, the registration processing will determine the positions of the same point in other images. Over the years, a broad range of techniques have been developed for the various types of data and problems [23]. In this paper, we assume that the source images have already been registered.

We give a brief introduction to the normalized cuts algorithm for region segmentation in Section 2. In Section 3, the spatial frequency measure reflecting image clarity is introduced. In Section 4, the proposed algorithm is presented. Experimental results are presented in Section 5. Finally, in Section 6 the concluding remarks are given.

2. Region segmentation using normalized cuts

The idea of graph-based image segmentation is that the set of points are represented as a weighted undirected graph $\mathbf{G} = (\mathbf{V},\mathbf{E})$, where the nodes of the graph are the points in the image [21]. Every pair of nodes are connected by an edge, and the weight on each edge $\mathbf{W}(i,j)$ is a function of the similarity between nodes i and j. The graph $\mathbf{G} = (\mathbf{V},\mathbf{E})$ is segmented into two disjoint sets A and $B = V - A$, by cutting the edges connecting the two parts. The degree of dissimilarity between the two parts is the total weight of edges cut.

Instead of using the value of total edge weight connecting the two partitions, Shi and Malik proposed a disassociation measure to compute the cut cost as a fraction of the total edge connections to all the nodes in the graph [21]. It is called the normalized cut (Ncut):

$$\mathrm{Ncut}(A,B) = \frac{\mathrm{cut}(A,B)}{\mathrm{assoc}(A,V)} + \frac{\mathrm{cut}(A,B)}{\mathrm{assoc}(B,V)}, \tag{1}$$

where $\mathrm{cut}(A,B) = \sum_{u\in A, t\in B} w(u,t)$ is the total connection from nodes in A to nodes in

B,$\mathrm{assoc}(A,V) = \sum_{u\in A, t\in V} w(u,t)$ is the total connection from nodes in A to all nodes in the graph and $\mathrm{assoc}(B,V)$ is similarly defined.

The algorithm is summarized as follows, assuming that the image **I** is to be segmented.

(1) Define the feature description matrix for a given image and a weighting function
(2) Set up a weighted graph $\mathbf{G} = (\mathbf{V},\mathbf{E})$, compute the edge weights and summarize information into **W** and **D** where the matrix **W** is represented as following.

$$\mathbf{W}(i,j) = \mathrm{e}^{\frac{-\|\mathbf{F}(i)-\mathbf{F}(j)\|_2^2}{\sigma_I^2}} * \begin{cases} \mathrm{e}^{\frac{-\|\mathbf{X}(i)-\mathbf{X}(j)\|_2^2}{\sigma_X^2}} & \text{if} \|X(i)-X(j)\|_2 < \mathbf{r} \\ 0 & \text{otherwise} \end{cases} \quad (2)$$

where $\mathbf{X}(i)$ is the spatial location of node i, and $\mathbf{F}(i) = \mathbf{I}(i)$, is the intensity value. If nodes i and j are more than r pixels away, $\mathbf{W}(i,j)$ will be zero. Generally, the value of σ is set to 10 to 20 percent of the total range of the feature distance function. The matrix **D** is a $N \times N$ diagonal matrix with $\boldsymbol{d}(i) = \sum_j \mathbf{W}(i,j)$ on its diagonal.

(3) Solve $(\mathbf{D} - \mathbf{W})\mathbf{x} = \lambda \mathbf{D}\mathbf{x}$ for eigenvectors with the smallest eigenvalues.
(4) Use the eigenvector with second smallest eigenvalue to bipartition the graph by finding the splitting points so that Ncut is minimized.
(5) Decide whether the current partition is stable and check the value of the resulting Ncut. The stability criterion is defined to measure the degree of smoothness in the eigenvector values. The simplest definition is based on first computing the histogram of the eigenvector values and then computing the ratio between the minimum and maximum values in the bins. In our experiments, we set a threshold on the ratio described above. The eigenvector which is smaller than the threshold is unstable. The value is set to be 0.06 in all our experiments. If the current partition should be subdivided, recursively repartition the segmented parts (go to step 2), otherwise exit.

3. Spatial frequency

The spatial frequency, which originated from the human visual system, indicates the overall active level in an image. The human visual system is too complex to be fully understood with present physiological means, but the use of spatial frequency has led to an effective objective quality index for image fusion [24]. The spatial frequency of an image block is defined as follows:

Consider an image of size $M \times N$, where M equals the number of rows and N the number of columns. The row (RF) and column (CF) frequencies of the image block are given by

$$\mathrm{RF} = \sqrt{\frac{1}{MN}\sum_{m=0}^{M-1}\sum_{n=1}^{N-1}[\mathbf{F}(m,n) - \mathbf{F}(m,n-1)]^2} \quad (3)$$

where $\mathbf{F}(m,n)$ is the gray value of pixel at position (m,n) of image F.

$$\mathrm{CF} = \sqrt{\frac{1}{MN}\sum_{n=0}^{N-1}\sum_{m=1}^{M-1}[\mathbf{F}(m,n) - \mathbf{F}(m-1,n)]^2} \quad (4)$$

The total spatial frequency of the image is then

$$\mathrm{SF} = \sqrt{(\mathrm{RF})^2 + (\mathrm{CF})^2}. \quad (5)$$

4. Multifocus image fusion using regions' clarity

Fig. 2 shows the schematic diagram of the proposed multifocus image fusion method. We assume that there are two multifocus source images for simplicity. The condition with three or more source images will be discussed later.

The fusion process is accomplished by the following steps.

(1) The temporary fused image is obtained by averaging two registered source images A and B.

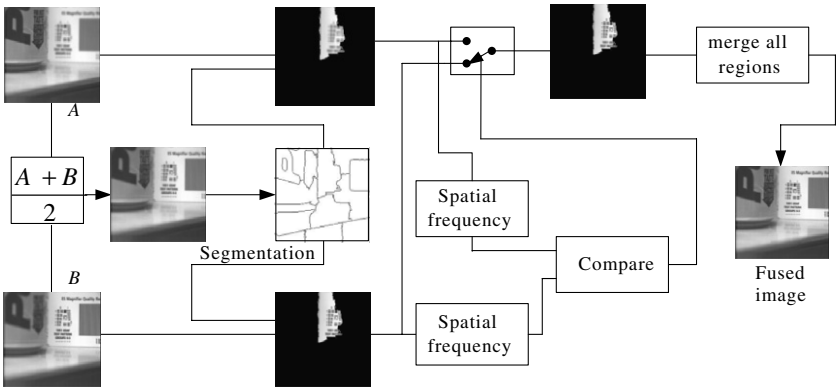

Fig. 2. Schematic diagram of the proposed image fusion method.

(2) The temporary fused image is segmented into several regions using the normalized cuts algorithm.
(3) Partition image A and B using the result of step (2).
(4) The spatial frequency of each region of segmented A and B is computed.
(5) Compare the spatial frequency of the corresponding regions of the two source images to decide which should be used to construct the fused image:

$$\mathrm{RoF}_i = \begin{cases} \mathrm{RoA}_i & \mathrm{SF}_i^A \geqslant \mathrm{SF}_i^B \\ \mathrm{RoB}_i & \mathrm{SF}_i^A < \mathrm{SF}_i^B \end{cases} \quad (6)$$

where RoF_i is the ith region of the fused image, SF_i^A and SF_i^B are the spatial frequencies of the ith region of image A and B, respectively.
(6) Merge all the selected regions to reconstruct the final image.
If there are three or more source images, partition all the source images using the result of step (2), then calculate the spatial frequency of each region. Select the region with maximum spatial frequency. Finally, merge all the regions to reconstruct the fused image as step (6).

5. Experimental results

The multifocus images shown in Figs. 3 and 4 are used to compare the proposed method and the technique based on the wavelet transform. In Fig. 3(a) and (b) the focus is on the Pepsi can and the testing card, respectively. Figs. 4(a) and (b) focus on the student and clock, respectively.

For the wavelet-based fusion method, Daubechies 'db1' and a decomposition level of 3 were used. Region-based activity measurement is employed to reflect the active level of decomposed coefficients. The coefficients are combined by choosing the maximum value. Window-based verification is applied to consistency verification. These three selection methods are optimal according to the experimental results in [9].

Fusion results using the proposed algorithm and wavelet-based approach are shown in Figs. 3 and 4. Fig. 3(c) is the fused result by using simple averaging. The segmented image using normalized cuts algorithm is shown in Fig. 3(d). The parameter setting is $\sigma_I = 0.1$, $\sigma_X = 0.3$, $r = 10$. From the segmented results, we can see that the regions with different focus measures are segmented correctly. Fig. 3(e) and (f) are the fused results by using the wavelet approach and the proposed method, respectively. To make better comparisons, the difference images between the fused image and the source images are given in Fig. 3(g)–(j). For the focused regions, the difference between the source image and the fused image should be zero. For example, in Fig. 3(a) the Pepsi can is clear, and in Fig. 3(h) the difference between Fig. 3(f) and (a) in the Pepsi can region is slight. This demonstrates that the whole focused area is contained in the fused image successfully. However, the difference between

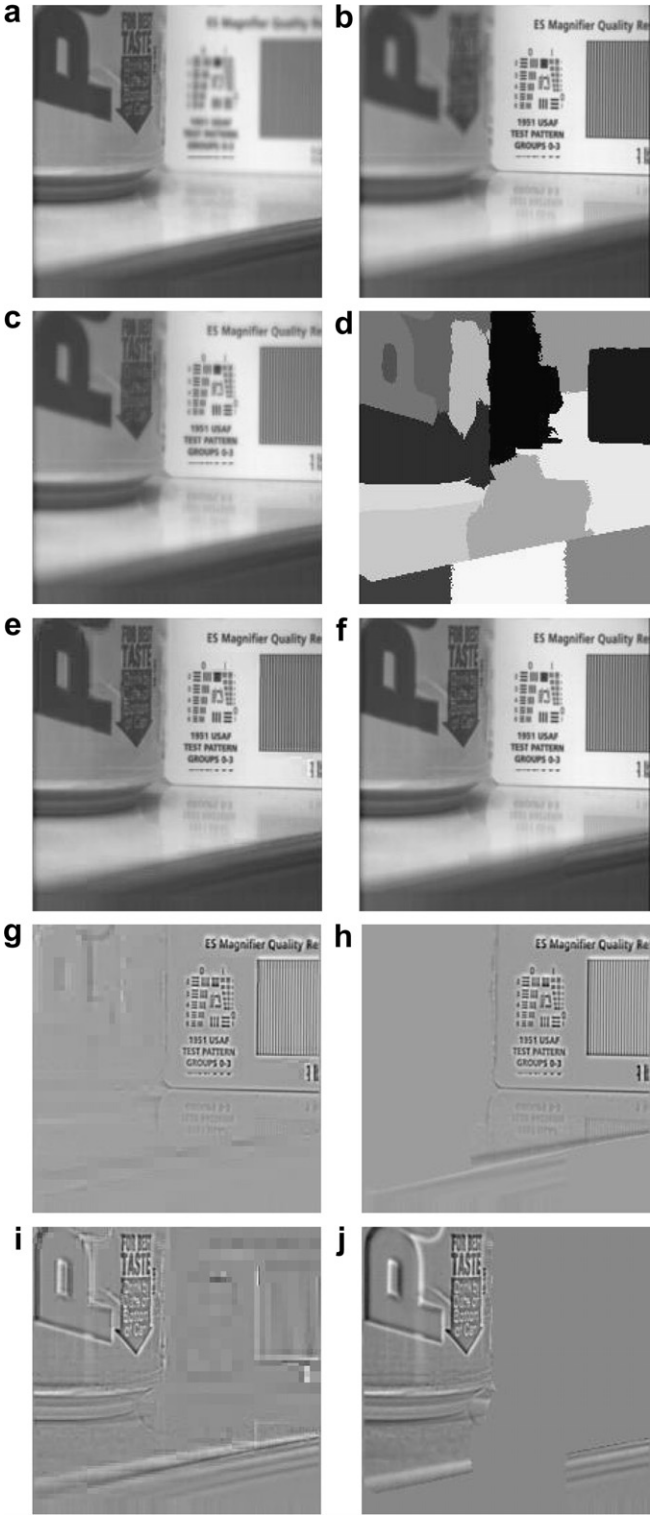

Fig. 3. Source images and fusion results: (a) Image focused on the Pepsi can. (b) Image focused on the testing card. (c) Temporal fused image using average method. (d) The segmented image. (e) Fused image using wavelet transform. (f) Fused image using the proposed algorithm. (g) Difference between (e) and (a). (h) Difference between (f) and (a). (i) Difference between (e) and (b). (j) Difference between in (f) and (b).

Fig. 3(e) and (a) in the same region shown in Fig. 3(g) is greater, which shows that the fused result using wavelets is worse than that of our proposed method. In Fig. 4, the same

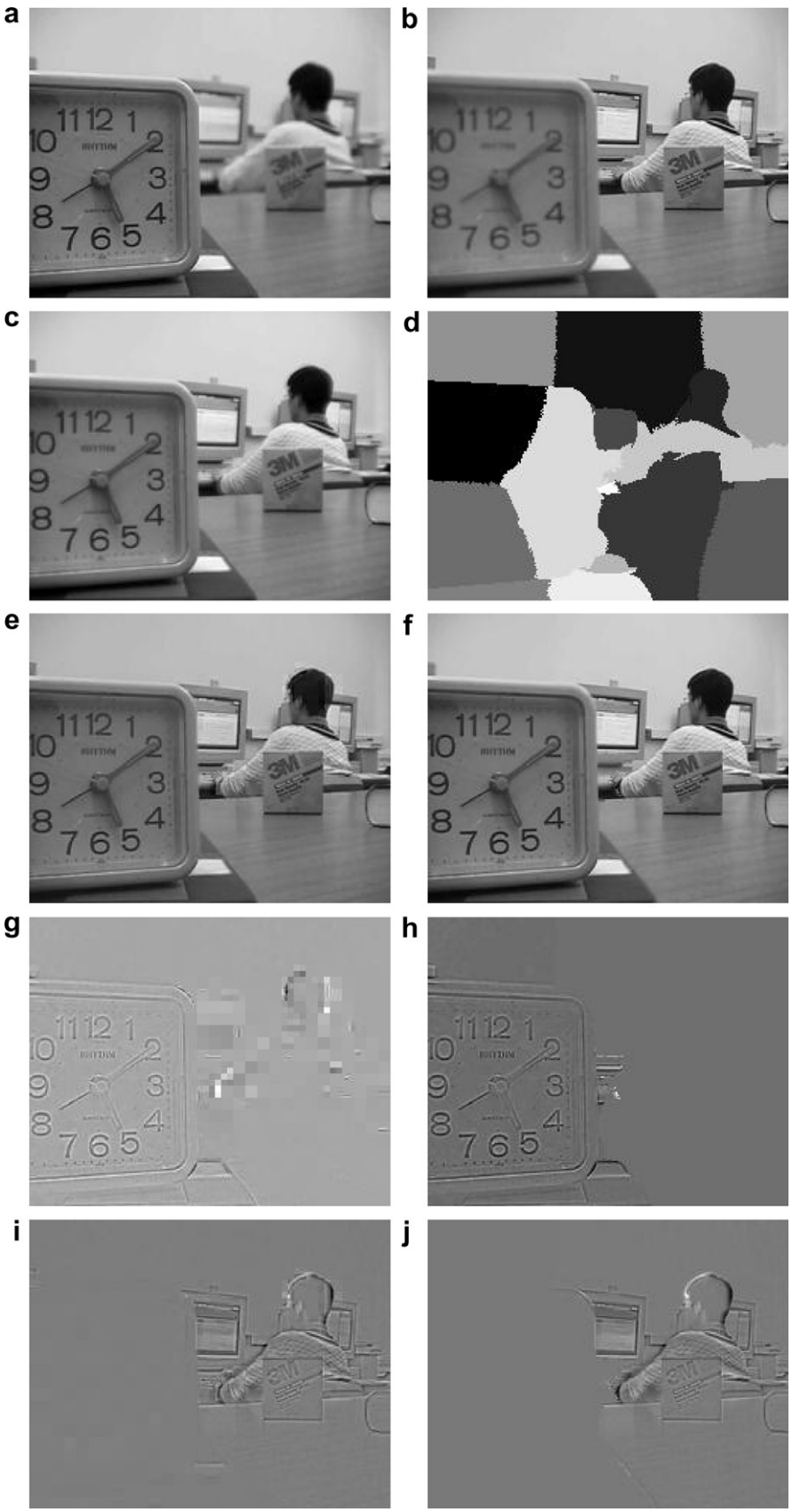

Fig. 4. (a) Image focused on the student. (b) Image focused on the clock. (c) Temporal fused image using average method. (d) The segmented image. (e) Fused image using wavelet transform. (f) Fused image using the proposed algorithm. (g) Difference between (e) and (a). (h) Difference between (f) and (a). (i) Difference between (e) and (b). (j) Difference between in (f) and (b).

conclusion can be drawn that the proposed method outperforms the wavelet transform approach.

Another two examples with three source images are presented in Figs. 5 and 6. They have similar results as previous examples.

For further comparison, two objective criteria are used to compare the fusion results. The first criterion is the $Q^{AB/F}$ metric, proposed by Xydeas and Petrovic in [25,26], which considers the amount of edge information transferred from the input images to the fused images. This

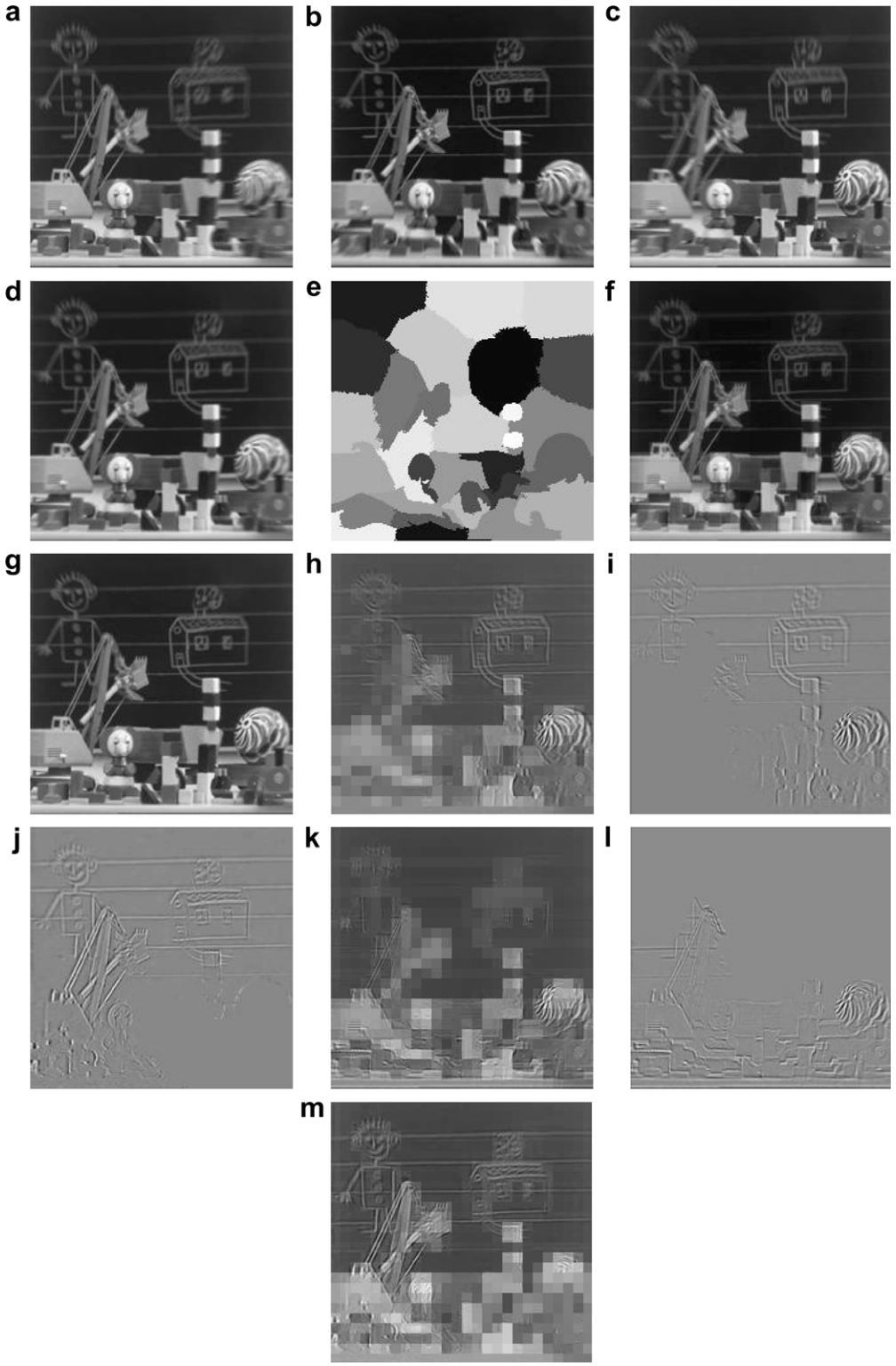

Fig. 5. (a)–(c) Three source image with different focus. (d) Temporal fused image using average method. (e) The segmented image. (f) Fused image using wavelet transform. (g) Fused image using the proposed algorithm. (h) Difference between (f) and (a). (i) Difference between (g) and (a). (j) Difference between (f) and (b). (k) Difference between in (g) and (b). (l) Difference between (f) and (c). (m) Difference between in (g) and (c).

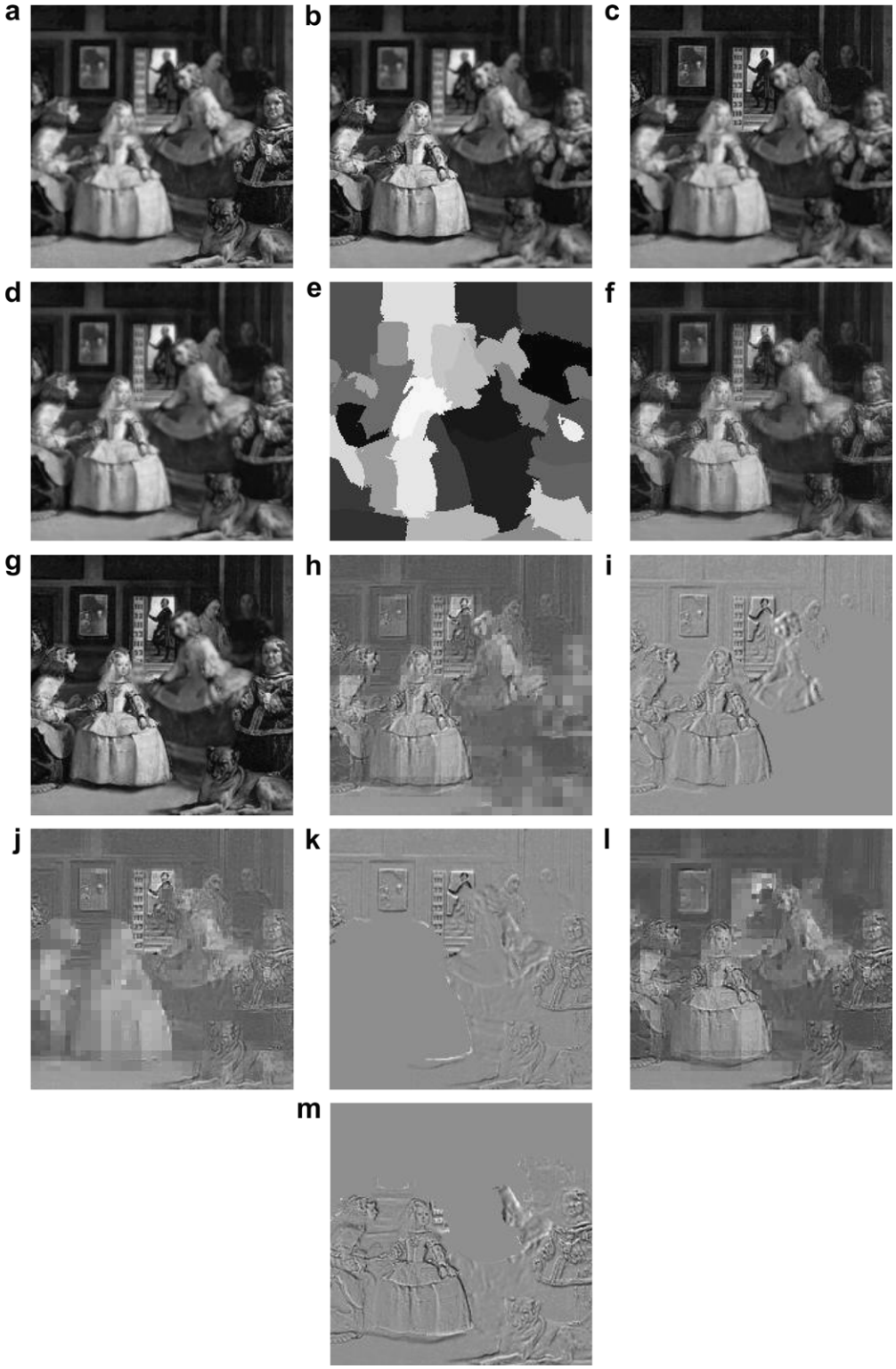

Fig. 6. (a)–(c) Three source image with different focus. (d) Temporal fused image using average method. (e) The segmented image. (f) Fused image using wavelet transform. (g) Fused image using the proposed algorithm. (h) Difference between (f) and (a). (i) Difference between (g) and (a). (j) Difference between (f) and (b). (k) Difference between in (g) and (b). (l) Difference between (f) and (c). (m) Difference between in (g) and (c).

method uses a Sobel edge detector to calculate the strength and orientation information at each pixel in both source and fused images. For two input images A and B, and a resulting fused image F, the Sobel edge operator is applied to yield the edge strength $g(n,m)$ and orientation $\alpha(n,m)$ information for each pixel as:

Table 1
Performance of different fusion methods

Source images	$Q^{AB/F}$		MI	
	Proposed method	DWT	Proposed method	DWT
Fig. 3	0.7593	0.7298	9.6280	7.4741
Fig. 4	0.7466	0.7237	9.1661	7.7328
Fig. 5	0.7206	0.6646	11.5460	8.5458
Fig. 6	0.5631	0.4916	9.8936	7.2884

$$g_A(n,m) = \sqrt{s_A^x(n,m)^2 + s_A^y(n,m)^2} \tag{7}$$

$$\alpha_A(n,m) = \tan^{-1}\left(\frac{s_A^y(n,m)}{s_A^y(n,m)}\right) \tag{8}$$

where $s_A^x(n,m)$ and $s_A^y(n,m)$ are the output of the horizontal and vertical Sobel templates centered on pixel $p_A(n,m)$ and convolved with the corresponding pixels of image A. The relative strength and orientation values of an input image A with respect to F are formed as:

$$\left(G_{n,m}^{AF}, A_{n,m}^{AF}\right) = \left(\left(\frac{g_{n,m}^F}{g_{n,m}^A}\right)^M, 1 - \frac{|\alpha_A(n,m) - \alpha_F(n,m)|}{\pi/2}\right) \tag{9}$$

where $M = \begin{cases} 1 & \text{if } g_A(n,m) > g_F(n,m) \\ -1 & \text{otherwise} \end{cases}$.

Edge information preservation values are then defined as:

$$Q_{n,m}^{AF} = \Gamma_g \Gamma_\alpha \left(1 + e^{k_g(G_{n,m}^{AF} - \sigma_g)}\right)^{-1} \left(1 + e^{k_\alpha(A_{n,m}^{AF} - \sigma_\alpha)}\right)^{-1} \tag{10}$$

Finally, the $Q^{AB/F}$ is defined as

$$Q^{AB/F} = \frac{\sum_{\forall n,m} Q_{n,m}^{AF} w_{n,m}^A + Q_{n,m}^{AF} w_{n,m}^B}{\sum_{\forall n,m} w_{n,m}^A + w_{n,m}^B}, \tag{11}$$

which evaluates the sum of edge information preservation values for both inputs Q^{AF} and Q^{BF} weighted by local importance perceptual factors w^A and w^B. We defined $w^A(n,m) = [g_A(n,m)]^L$ and $w^B(n,m) = [g_B(n,m)]^L$. L is a constant. For the "ideal fusion", $Q^{AB/F} = 1$.

The second criterion is mutual information (MI) [27]. It is a metric defined as the sum of mutual information between each input image and the fused image. Considering two input images A and B, and a resulting fused image F:

$$I_{FA}(f,a) = \sum_{f,a} p_{FA}(f,a) \log \frac{p_{FA}(f,a)}{p_F(f) p_A(a)} \tag{12}$$

$$I_{FB}(f,b) = \sum_{f,b} p_{FB}(f,b) \log \frac{p_{FB}(f,b)}{p_F(f) p_B(b)} \tag{13}$$

Thus the image fusion performance measure can be defined as

$$MI_F^{AB} = I_{FA}(f,a) + I_{FB}(f,b) \tag{14}$$

which indicates that the proposed measure reflects the total amount of information that the fused image F contains that of A and B. For both criteria, the larger the value, the better is the fusion result.

The values of $Q^{AB/F}$ and MI of Figs. 3–6 are listed in Table 1. We observe that the proposed scheme provides better performance and outperforms the discrete wavelet transform approach in terms of $Q^{AB/F}$ and MI. A shortcoming of our method is that it consumes more time than the wavelet based methods because the segmentation process is time-consuming.

6. Conclusions

In this paper, a new region-based multifocus image fusion method is proposed. There are a number of advantages of region based image fusion, including: (1) Region based image fusion methods process regions rather than individual pixels, which is helpful to overcome some of the problems existing in pixel-fusion methods such as sensitivity to noise, blurring effects and mis-registration; (2) Using feature to represent the image information not only reduces the complexity of the procedure but also increases the reliability of fusion results; (3) Fusion rules are based on combining groups of pixels which form an image region. The basic idea of our proposed method is to perform image segmentation using normalized cuts on an intermediate fused image, then the segmented regions are fused using spatial features. We have compared the results with the results of a wavelet based method. Experimental results on pairs and triples of images show that the better results are obtained.

Acknowledgements

The author thank the editor and anonymous reviewers for their detailed review, valuable comments and constructive suggestions. The author thank Dr. Xiaoyi Jiang for his helpful suggestions. This paper is supported by the National Natural Science Foundation of China (No. 60402024) and Program for New Century Excellent Talents in University (NECT-2005).

References

[1] J.K. Aggarwal, Multisensor Fusion for Computer Vision, Spinger-Verlag, Berlin, Germany, 1993.
[2] W.B. Seales, S. Dutta, Everywhere-in-focus image fusion using controllable cameras, Proceedings of SPIE 2905 (1996) 227–234.
[3] P.T. Burt, E.H. Andelson, The Laplacian pyramid as a compact image code, IEEE Transactions on Communications 31 (4) (1983) 532–540.
[4] P.J. Burt, A gradient pyramid basis for pattern selective image fusion, in: Proceedings of the Society for Information Display Conference, 1992, pp. 467–470.
[5] A. Toet, Image fusion by a ratio of low-pass pyramid, Pattern Recognition 9 (4) (1989) 245–253.
[6] G.K. Matsopoulos, S. Marshall, J. Brunt, Multiresolution morphological fusion of MR and CT images of the human brain, IEEE Proceedings – Vision, Image, and Signal Processing 141 (3) (1994) 137–142.
[7] H. Li, B.S. Manjunath, S.K. Mitra, Multisensor image fusion using the wavelet transform, Graphical Models and Image Processing 57 (3) (1995) 235–245.

[8] A.Y. David, Image merging and data fusion by means of the discrete two-dimensional wavelet transform, Journal of Optical Society of America (A) 12 (9) (1995) 1834–1841.
[9] Z. Zhang, R.S. Blum, A categorization of multiscale-decomposition-based image fusion schemes with a performance study for a digital camera application, Proceedings of IEEE 87 (8) (1999) 1315–1326.
[10] G. Pajares, J. Cruz, A wavelet-based image fusion tutorial, Pattern Recognition 37 (9) (2004) 1855–1872.
[11] S. Gabarda, G. Cristóbal, Cloud covering denoising through image fusion, Image and Vision Computing 25 (5) (2007) 523–530.
[12] I. De, B. Chanda, B. Chattopadhyay, Enhancing effective depth-of-field by image fusion using mathematical morphology, Image and Vision Computing 24 (12) (2006) 1278–1287.
[13] A. Goshtasby, Fusion of multi-exposure images, Image and Vision Computing 23 (6) (2005) 611–618.
[14] S. Li, J.T. Kwok, I.W. Tsang, Y. Wang, Fusing images with different focuses using support vector machines, IEEE Transactions on Neural Networks 15 (6) (2004) 1555–1561.
[15] S. Li and Y. Wang, Multisensor image fusion using discrete multiwavelet transform, in: Proceedings of the 3rd International Conference on Visual Computing, 2000, pp. 93–103.
[16] H. Wang, J. Peng, W. Wu, Fusion algorithm for multisensor images based on discrete multiwavelet transform, IEEE Proceedings – Vision, Image, and Signal Processing 149 (5) (2002) 283–289.
[17] I. De, B. Chanda, A simple and efficient algorithm for multifocus image fusion using morphological wavelets, Signal Processing 86 (5) (2006) 924–936.
[18] S.G. Nikolov, J.J. Lewis, R.J. O'Callaghan, D.R. Bull, C.N. Canagarajah, Hybrid fused displays: between pixel- and region-based image fusion, in: Proceedings of 7th International Conference on Information Fusion, Stockholm, Sweden, June 2004, pp. 1072–1079.
[19] G. Piella, A general framework for multiresolution image fusion: from pixels to regions, Information Fusion 4 (4) (2003) 259–280.
[20] J.J. Lewis, R.J. O'Callaghan, S.G. Nikolov, D.R. Bull, C.N. Canagarajah, Region-based image fusion using complex wavelets, in: Proceedings of 7th International Conference on Information Fusion, Stockholm, Sweden, June 2004, pp. 555–562.
[21] J. Shi, J. Malik, Normalized cuts and image segmentation, IEEE Transactions on Pattern Analysis and Machine Intelligence 22 (8) (2000) 888–905.
[22] A. Goshtasby, Fusion of multifocus images to maximize image information, Proceedings of the SPIE 6229 (2006) 21–30.
[23] L.G. Brown, A survey of image registration techniques, ACM Computing Surveys 24 (4) (1992) 325–376.
[24] S. Li, J.T. Kwok, Y. Wang, Combination of images with diverse focuses using the spatial frequency, Information Fusion 2 (3) (2001) 169–176.
[25] C. Xydeas, V. Petrovic, Objective image fusion performance measure, Electronics Letters 36 (4) (2000) 308–309.
[26] V. Petrovic, C. Xydeas, Sensor noise effects on signal-level image fusion performance, Information Fusion 4 (3) (2003) 167–183.
[27] G. Qu, D. Zhang, P. Yan, Information measure for performance of image fusion, Electronics Letters 38 (7) (2001) 313–315.